HHS Public Access

Author manuscript

Nat Cell Biol. Author manuscript; available in PMC 2012 March 01.

Published in final edited form as:

Nat Cell Biol. ; 13(9): 1108–1115. doi:10.1038/ncb2310.

RalA and RalBP1 regulate mitochondrial fission at mitosis

David F. Kashatus[1], **Kian-Huat Lim**[1,†], **Donita C. Brady**[1], **Nicole L.K. Pershing**[1], **Adrienne D. Cox**[2], and **Christopher M. Counter**[1,3]

[1]Department of Pharmacology and Cancer Biology, Department of Radiation Oncology, Duke University Medical Center, Durham, NC 27710

[2]Department of Radiation Oncology, Lineberger Comprehensive Cancer Center, University of North Carolina at Chapel Hill, Chapel Hill, NC 27599

Abstract

Mitochondria exist as dynamic interconnected networks that are maintained through a balance of fusion and fission[1]. Equal distribution of mitochondria to daughter cells during mitosis requires fission[2]. Mitotic mitochondrial fission depends upon both the relocalization of large GTPase Drp1 to the outer mitochondrial membrane and phosphorylation of S616 on Drp1 by the mitotic kinase cyclin B/Cdk1[2]. We now report that these processes are mediated by the small *Ra*s-*l*ike GTPase RalA and its effector RalBP1 (RLIP76/RLIP1/RIP1)[3,4]. Specifically, the mitotic kinase Aurora A phosphorylates S194 of RalA, relocalizing it to the mitochondria, where it concentrates RalBP1 and Drp1. Furthermore, RalBP1 associates with cyclin B/Cdk1 kinase activity to foster phosphorylation of Drp1 on S616. Disrupting either RalA or RalBP1 leads to a loss of mitochondrial fission at mitosis, improper segregation of mitochondria during cytokinesis and a decrease in ATP levels and cell number. Thus, the two mitotic kinases Aurora A and cyclin B/Cdk1 converge upon RalA and RalBP1 to promote mitochondrial fission, the appropriate distribution of mitochondria to daughter cells and ultimately proper mitochondrial function.

The mitotic kinase Aurora A phosphorylates S194 in the C-terminus of RalA[5], increasing the level of active GTP-bound RalA[5,6] and redistributing it from the plasma membrane to internal membranes[6]. The related protein KRas is also phosphorylated at the C-terminus by PKC, which relocalizes it from the plasma membrane to the mitochondria[7]. Given this, we tested and found that a portion of GFP-RalA co-localized with internal membranes stained with the dye MitoTracker Red[8] in human HEK-TtH[9] cells (Fig. 1a). Similarly, endogenous RalA was detected by immunoblot in a highly purified (complex Vβ-positive, calnexin, tubulin and Na^+/K^+ ATPase-negative) mitochondrial fraction (Fig. 1b). Moreover, RalA was enriched in the mitochondrial fraction upon expression of kinase active (T288D)[10], but not

---

[3]Correspondence: count004@mc.duke.edu.

[†]Current address: Medical Oncology Branch, National Cancer Institute, National Institutes of Health, Bethesda, MD 20892

Supplementary Information. A figure summarizing the main result of this paper is available in Supplementary Information.

Author Contributions Initial pilot experiments were performed by K.-H.L. and expanded upon by D.F.K., D.C.B. and N.L.K.P. All authors contributed to the study design. The manuscript was written by D.F.K. and C.M.C. with contributions by K.-H.L., D.C.B., N.L.K.P. and A.D.C.

inactive (K162R)[10] Aurora A (Fig. 1C). Similarly, an Aurora A phosphomimetic (S194D) version of RalA (Supplementary Fig. S2a), previously shown to be enriched in internal membranes[6], showed a marked increase in co-localization with mitochondria, whereas mutation of this phosphorylation site (S194A) decreased this co-localization (Fig. 1a). Taken together, these data suggest that phosphorylation of RalA by Aurora A results in the accumulation of RalA at mitochondria, or vesicles tightly associated with mitochondria[11].

Notably, Aurora A activity also had an effect on mitochondria morphology. While the majority of vector control cells exhibited a mix of interconnected and smaller, punctate mitochondria, most cells expressing Aurora A^{T288D} displayed small punctate or circular mitochondria, whereas most cells expressing Aurora A^{K162R}, which has been reported to exhibit dominant-negative activity[6,12], had long interconnected mitochondria (Fig. 1d). To further investigate this effect on mitochondrial dynamics, we analyzed the distribution of the large GTPase Drp1, which relocalizes from a diffuse cytoplasmic to a punctate mitochondrial distribution during mitochondrial fission[13]. Like RalA, the levels of Drp1 in the mitochondrial fraction increased in cells expressing Aurora A^{T288D}, but not Aurora A^{K162R} (Fig. 1c). Moreover, the $Drp1^{K38A}$ mutant that lacks GTPase activity and inhibits fission[14,15] reversed the fragmented mitochondrial phenotype induced by Aurora A^{T288D} (Supplementary Fig. S2b), arguing that Aurora A does not block fusion but instead promotes mitochondrial fission. Furthermore, while most cells over-expressing wild type RalA (Supplementary Fig. S2a) exhibited slightly more fragmented mitochondria than vector control cells (Fig. 1d), consistent with higher levels of RalA, expression of $RalA^{S194D}$ caused a significant shift away from this phenotype, with most cells instead characterized by a fragmented mitochondrial network (Fig. 1e). Similarly, the fragmented mitochondrial phenotype of cells expressing Aurora A^{T288D} was reversed if RalA was knocked down by RalA shRNA and replaced with shRNA-resistant $RalA^{S194A}$, but not wild type RalA (Supplementary Fig. S2c). Taken together, these data suggest that Aurora A promotes mitochondrial fission through phosphorylation of RalA on S194.

To assess whether loss of RalA results in fusion, we analyzed the mitochondrial morphology of HEK-TtH cells in which RalA was knocked down by shRNA and complemented with either an empty vector, shRNA-resistant wild type or S194A mutant RalA (Supplementary Fig. S2a). While scramble control cells had a mixture of short and long mitochondria (Fig. 1f), half of the cells expressing RalA shRNA exhibited long interconnected networks of mitochondria, with few cells having short punctate mitochondria (Fig. 1f). Knockdown of RalA also resulted in a roughly two-fold reduction in total Drp1 protein levels, but an 18-fold reduction in the level of Drp1 in the mitochondrial fraction (Fig. 1g). Furthermore, FRAP analysis of mitochondrial targeted YFP revealed that RalA knockdown cells had a significantly faster recovery following photobleaching than scramble controls (Fig. 1h, Supplementary Fig. S2d), indicating a more interconnected mitochondrial network[16]. This interconnected phenotype was reversed upon expression of shRNA-resistant wild type, but not S194A mutant RalA (Fig. 1f). Knockdown of the highly related RalB protein, which is not a target of Aurora A[5], did not affect mitochondrial morphology (Supplementary Fig. S3a). These loss-of-function experiments are in agreement with the described gain-of-function experiments, suggesting that Aurora A promotes mitochondrial fission through phosphorylation of RalA on S194.

In the active state, RalA binds effector proteins to mediate signaling[3,4]. In the presence of Aurora A, RalA preferentially co-immunoprecipitates with the multifunctional effector RalBP1 over the effectors Sec5 and Exo84[6]. Given this, whole cell and purified mitochondrial extracts isolated from HEK-TtH cells expressing vector control, active (T288D) or inactive (K162R) Aurora A were immunoblotted to ascertain the subcellular localization of endogenous RalBP1. While the level of RalBP1 in whole cell extracts was similar in each cell line, it was increased two-fold in the mitochondrial fraction of cells expressing Aurora A^{T288D} compared to cells expressing vector or Aurora A^{K162R} (Fig. 2a). Furthermore, while total RalBP1 levels were unaffected by the presence or absence of RalA, there was a greater than two-fold reduction in the levels of RalBP1 in the mitochondrial fraction upon knockdown of RalA. Conversely, knockdown of RalBP1 had no effect on the amount of RalA in the mitochondrial fraction (Fig. 2b). Like RalA, knockdown of RalBP1 also led to a significant increase in the number of cells with long interconnected networks of mitochondria and a relative absence of short punctate mitochondria compared to scramble control cells (Fig. 2c); an effect that was reversed by expression of shRNA-resistant RalBP1 (Supplementary Fig. S2a, Fig. 2c). Conversely, knockdown of the RalA effector Sec5 resulted in, if anything, a decrease in elongated mitochondria (Supplementary Fig. S3a). Furthermore, knockdown of RalBP1 in cells expressing Aurora A^{T288D} reduced both the number of these cells with short, punctate or circular mitochondria (Fig. 2d), nearly to the level observed in control cells (Fig. 1d), and reduced the levels of Drp1 in the mitochondrial fraction (Fig. 2e). Both of these effects were reversed by expression of an shRNA-resistant version of RalBP1 (Fig. 2d,e). Taken together, these data suggest that when RalA is phosphorylated by Aurora A, it is enriched at mitochondria with RalBP1, which promotes recruitment of Drp1 and mitochondrial fission.

To test whether RalA-mediated recruitment of RalBP1 to mitochondria is sufficient to induce mitochondrial fission, RalBP1 was fused in frame with the C-terminal 30 amino acids of RalA (RalBP1-RalA), which contains S194 and imparts the polarized membrane delivery function and transforming activity of RalA to RalB[17,18] (Fig. 1e, Supplementary Fig. S2c). GFP-RalBP1-RalA in the phosphomimetic S194D configuration primarily co-localized with the mitochondria, while GFP-RalBP1-$RalA^{S194A}$ did not, despite widespread staining in the cell (Fig. 2f). Similarly, biochemical analysis revealed that more Myc-RalBP1-$RalA^{S194D}$ was present in the mitochondrial fraction compared to Myc-RalBP1-$RalA^{S194A}$ (Fig. 2g). Consistent with these results, almost half of the cells expressing Myc-RalBP1-$RalA^{S194D}$ exhibited small discrete and circular mitochondria (Fig. 2h) and had higher levels of mitochondrial Drp1 (Fig. 2g) similar to cells expressing Aurora A^{T288D} or $RalA^{S194D}$ (Fig. 1d,e). Conversely, cells expressing RalBP1-$RalA^{S194A}$ typically had elongated mitochondria (Fig. 2h) and lower levels of mitochondrial Drp1 (Fig. 2g), similar to knockdown of RalA or RalBP1 (Fig. 1f,2c), suggesting RalBP1-$RalA^{S194A}$ has dominant-negative activity, perhaps through sequestration of factors involved in promoting fission. These experiments support the notion that the localization of RalBP1 to mitochondria, through its association with phosphorylated RalA, is sufficient to recruit Drp1 to the mitochondria and drive fragmentation.

While RalA is a known substrate of Aurora A[5,6], phosphorylation of RalA by Aurora A during mitosis had not been described. HeLa cells, which can be readily synchronized and

have previously been used to study mitotic mitochondrial dynamics[2], were therefore engineered to express RalA or the phosphorylation-deficient mutant RalA^{S194A} and either left unsynchronized or synchronized and then collected at M-phase. Analysis of immunoprecipitated RalA by immunoblot with a phospho-S194 specific antibody showed that phosphorylation of RalA was higher in mitotic cells (cyclin B-positive) compared with unsynchronized controls (Fig. 3a), but was abolished in immunoprecipitates of RalA^{S194A} (Supplementary Fig. S3b). In addition, RalA, RalBP1, and Drp1 all accumulated in the mitochondrial fraction of M-phase cells, but not unsynchronized controls (Fig. 3b). Moreover, the enrichment of Drp1 in the mitochondrial fraction of M-phase (cyclin B and phospho-histone H3-positive) cells was reduced if either RalA, RalBP1, or Aurora A were knocked down (Fig. 3c,d and Supplementary Fig. S3d). This reduction did not result from a delay in M-phase entry, as levels of phospho-histone H3 (S10), a marker of mitotic cells, were elevated normally in each cell line (Supplementary Fig. 3c,d). Moreover, knockdown of Mff1, but not Fis1 (Supplementary Fig. S3e), reduced the mitochondrial recruitment of both RalBP1 and Drp1 at mitosis (Fig. 3e,f), consistent with Mff1, and not Fis1, being the primary protein involved in mitochondrial recruitment of Drp1 in mammalian cells[19]. Knockdown of Plk1 (Supplementary Fig. S3e), another target of Aurora A that mediates many of its mitotic effects[20], had no effect on the mitochondrial levels of RalBP1 or Drp1 (Fig. 3f). These data suggest that Aurora A, RalA, and RalBP1 are required for recruitment of Drp1 to mitochondria during M-phase.

In addition to mitochondrial recruitment of Drp1, mitotic mitochondrial fission also requires phosphorylation of Drp1 on S616 by the mitotic kinase cyclin B/Cdk1[2]. Therefore, RalA and RalBP1 were knocked down in HeLa cells and the levels of total and S616 phosphorylated Drp1 were analyzed by immunoblot. Interestingly, knockdown of RalBP1, but not RalA, reduced the amount of phosphorylated Drp1 compared to scramble control cells (Fig. 4a). As RalBP1 binds cyclin B/Cdk1 and promotes phosphorylation of Epsin during mitosis[21], we tested whether Drp1-specific cyclin B/Cdk1 activity immunoprecipitated with RalBP1 from mitotic cell extracts. Immunoblot analysis confirmed that both cyclin B and S616 phosphorylated Drp1 were increased in M-phase versus unsynchronized extracts. The immunoprecipitates of cyclin B or RalBP1, but not a control immunoprecipitate, phosphorylated recombinant GST-Drp1$^{518–736}$, and moreover, this kinase activity was increased in M-phase extracts compared to unsynchronized extracts (Fig. 4b). Furthermore, RalBP1 immunoprecipitated with cyclin B from M-phase extracts (Fig. 4b). Based on these results, we speculate that RalBP1, through its interaction with cyclin B, acts as a scaffold to foster cyclin B/Cdk1 phosphorylation of Drp1 at mitosis. In agreement, addition of GST-RalBP1, but not control GST, led to a dose-dependent increase in S616 phosphorylation of recombinant GST-Drp1$^{518–736}$ by GST-cyclin B/Cdk1 *in vitro*, as measured both by autoradiography of ^{32}P-labeled GST-Drp1$^{518–736}$ and by immunoblot with a phospho-S616-specific antibody (Fig. 4c). Thus, RalBP1 promotes cyclin B/Cdk1 phosphorylation of Drp1 at mitosis independently of RalA. RalBP1 complexed with cyclin B/Cdk1 and Drp1 is, in turn, tethered to mitochondria through RalA. Indeed, immunoprecipitation of endogenous RalA from the mitochondrial fraction of HeLa cells collected at M-phase and treated with Dithiobis[succinimidyl propionate] to cross-link closely associated proteins revealed a complex including RalA, RalBP1, Drp1 and cyclin B

(Fig. 4d). Taken together, we propose that RalBP1 acts as a scaffold to bring cyclin B/Cdk1 in proximity to Drp1 to promote Drp1 phosphorylation on S616. RalBP1 also localizes this active Drp1 complex to mitochondria though its association with RalA, which is targeted to the mitochondria *vis-à-vis* phosphorylation on S194 by Aurora A (Supplementary Fig. S1).

During mitosis, extensive mitochondrial fission occurs during prophase, and mitochondria reform an interconnected network following cytokinesis[2]. Given the convergence of the two mitotic kinases Aurora A and cyclin B/Cdk1 on RalA and RalBP1, and the role RalA and RalBP1 play in mitochondrial morphology, we assessed whether RalA and RalBP1 are required for mitotic mitochondrial fission. To that end, we used time-lapse video microscopy to monitor mitotic mitochondrial morphology, visualized by a mitochondrial targeted red fluorescent protein, of HeLa cells stably expressing scramble, RalBP1, or RalA shRNA. Compared to scramble control cells, the mitochondria of cells in which either RalA or RalBP1 were knocked down retained an interconnected morphology throughout mitosis, which in some cells resulted in mitochondrial bridges during cytokinesis (Fig. 5a, Supplementary Movies 1–6) and unequal partitioning of mitochondria between mother and daughter cells (Fig. 5a, Supplementary Movies 1–6). In some cells cytokinesis was also disrupted, perhaps a consequence of a failure to segregate mitochondria correctly, although RalA may also play a more direct role in this process[22]. To more closely investigate these mitotic phenotypes, mitochondria from HeLa cells expressing a scramble, RalBP1, or RalA shRNA alone or in conjunction with shRNA-resistant $RalA^{WT}$ or $RalA^{S194A}$ (Fig. 5b,c) were analyzed by confocal microscopy throughout each stage of mitosis, defined by the condensation and positioning of DAPI-stained chromosomes. Consistent with the live cell imaging and with previous reports[2], scramble control HeLa cells exhibited significant mitochondrial fragmentation beginning at prophase and lasting through to telophase (Fig. 5b). In contrast, mitochondria in RalA or RalBP1 knockdown cells did not undergo fragmentation, but instead maintained a netlike appearance throughout mitosis (Fig. 5b). To quantitate this effect, the number of cells with an extended network of mitochondria at metaphase was measured, revealing that knockdown of either RalA or RalBP1 more than doubled the number of cells with this mitochondrial morphology (Fig. 5d). Notably, expression of shRNA-resistant wild type RalA, but not $RalA^{S194A}$, rescued the effect of RalA shRNA on mitochondrial morphology, restoring the normal fragmentation of mitochondria at metaphase (Fig. 5c,d). Stable expression of Aurora A^{K162R} also nearly doubled the number of cells exhibiting netlike mitochondria during metaphase compared to scramble control cells (Supplementary Fig. S3f). These data suggest that Aurora A promotes mitochondrial fission at mitosis through RalA and RalBP1.

The loss of mitochondrial fission is associated with mitochondrial dysfunction, including impaired energy production[23,24]. Intriguingly, compared to scramble control HeLa cells, knockdown of RalA or RalBP1 (Fig. 3c) significantly lowered the levels of cellular ATP (Fig. 5e) and eventually led to a decrease in the number of metabolically active cells (Fig. 5f). Such an effect could be the consequence of successive rounds of unequal distribution of mitochondria during cell division, and indeed disruption of fission has been reported to decrease mtDNA levels over time[24], but could also be the result of either a defect in the

clearing of damaged mitochondria or in the ability of functional mitochondria to complement damaged mitochondria through content mixing[1].

Normal cell division requires coordinated and equal distribution of a vast amount of cellular material between the two daughter cells. In this regard, we now propose that during mitosis, Aurora A phosphorylates RalA at S194, redistributing a fraction of this protein and its effector RalBP1 to mitochondria, or vesicles associated with mitochondria. Coordinately, RalBP1 enhances the phosphorylation of Drp1 on S616 by the mitotic kinase cyclin B/Cdk1 and through its association with RalA, promotes Drp1 recruitment to mitochondria, fission, and proper segregation of mitochondria during cell division, which helps maintain proper mitochondrial and cellular function (Supplementary Fig. S1).

Methods

Plasmids

pSuper-Retro-Puro plasmids encoding RalA shRNA, RalB shRNA, RalBP1 shRNA, or a scramble sequence, pSuper-Retro-Puro-TetO encoding scramble or Aurora A shRNA, pBabe-Bleo encoding HA epitope-tagged Aurora A^{K162R} and Aurora A^{T288D}, pBabe-Neo encoding shRNA-resistant Myc epitope-tagged RalA, pBabe-Puro encoding shRNA-resistant Flag epitope-tagged RalA, GFP-tagged RalA, $RalA^{S194D}$ and $RalA^{S194A}$, and pCMV-Neo Tet Repressor were described previously[6,17,25]. shRNA sequences targeting Sec5 (5'-GGGTGATTATGATGTGGTT-3')[26], Mff1 (5'-AACGCTGACCTGGAACAAGGA-3')[19], Fis1 (5'-AGGCATCGTGCTGCTCGAG-3')[27] and Plk1 (5'-GGAGGTGTTCGCGGGCAAG-3')[28] were cloned into pSuper-Retro-Puro. GST-RalBP1 and GST-$Drp1^{518–736}$ expression vectors were created by subcloning RalBP1 from pBabe-Puro RalBP1, and the fragment encoding amino acids 518 to 736 of Drp1 from the plasmid pcDNA3.1-flag-Drp1[29], into pGEX-5X2. The last 30 amino acids of $RalA^{S194A}$ or $RalA^{S194D}$ were fused in frame to the C-terminus of RalBP1 in pBabe-Puro-myc-RalBP1 and further subcloned into pEGFP-C2 to generate GFP-RalBP1-$RalA^{S194A}$ and GFP-RalBP1-$RalA^{S194D}$. pBabe-Puro-$Drp1^{K38A}$ was generated by subcloning $Drp1^{K38A}$ from pcDNA3.1-flag-$Drp1^{K38A}$ [29].

Cell culture

Transgenes and shRNA were either stably introduced into human HEK-TtH[9,17] or HeLa (ATCC) cells by retroviral infection as previously described[30] or, for GFP fusion constructs, were transiently introduced using the Fugene6 reagent (Roche). For synchronization, HeLa cells were treated with 2mM thymidine for 19 h, released in DMEM for 9 h, treated with 2mM thymidine for 15 h, released in DMEM for 10 h (10.5 h for Aurora A shRNA) and subjected to immunofluorescence to visualize mitochondria or harvested for immunoblot analysis[2]. To inducibly knock down Aurora A, HeLa cells stably expressing Tet Repressor (TR) and pSuper-Retro-Puro-TetO scramble or Aurora A shRNA were treated with 10μg/mL doxyxycline (sigma) for 10 h prior to cell harvest.

Protein analysis

Whole cell lysates were prepared in RIPA buffer (1% NP-40, 20 mM Tris pH 8.0, 137 mM NaCl, 10% glycerol, 2mM EDTA), and either resolved by SDS-PAGE or subjected to immunoprecipitation with 5μg of α-Cyclin B, α-RalBP1 (Santa Cruz) or α-myc (Cell Signaling Technologies) antibodies[6] and resolved by SDS-PAGE. For mitochondrial fractions[31], cells were resuspended in hypotonic lysis buffer (20 mM HEPES-KOH, pH 7.5, 10 mM KCl, 1.5 mM MgCl2, 1 mM EDTA, 1 mM EGTA, 250 mM sucrose, 1 mM dithiothreitol), on ice for 1 hour, then lysed with 125 strokes of a Teflon homogenizer. Homogenates were centrifuged at 750*g* and the supernatant was centrifuged at 10,000*g* to separate the cytoplasmic fraction (supernatant) and the heavy membrane fraction (pellet). The heavy membrane fraction was either lysed in RIPA (crude mitochondria) or resuspended in mitochondrial isolation buffer (MIB: 840 mM mannitol, 240 mM sucrose, 40 mM KCl, 1 mM succinate, 0.5 mM EDTA, 0.5 mM EGTA), and centrifuged over a discontinuous Percoll gradient (0, 25, 30, 37, 42%) for 25 min at 25,000 RPM. Highly purified mitochondria were recovered from the 37–42% interface and resuspended in 1 volume of RIPA buffer. Proteins for immunoblot were quantitated by Bradford assay (Bio-Rad), equivalent protein amounts (50 or 100μg) were resolved by SDS-Page, and immunoblotted with α-RalBP1 (Novus), α-RalA, α-Plk-1 (T210), α-Drp1 (BD Transduction Laboratories), α-S616-Drp1, α-Na^+/K^+-ATPase, α-Cdk1, α-S10-Histone H3, α-Histone H3 (Cell Signaling Technology), α-Complex V-β (Molecular Probes), α-calnexin (Stressgen), α-HA (Roche), α-RalB (Millipore), α-Cyclin B, α-Fis1 (Santa Cruz), β-actin, α-MFF or α-tubulin (Sigma). All antibody dilutions were 1:1000 except α-Cyclin B, α-Fis1, α-Cdk1, α-Drp1 and α-S616-Drp1 at 1:500.

Generation of phospho-S194 RalA antibody

Polyclonal anti-phospho-S194 antibody was generated by Open Biosystems according to the following protocol: 500μg KLH-conjugated phospho-peptide corresponding to S194 phosphorylated RalA (CGKKKRK[pS]LAKRIRE) was injected subcutaneously into 10 sites of two New Zealand white rabbits on day 1 followed by booster injections of 250μg into 4 sites/rabbit on days 14, 28 and 42. Production bleeds of 50 mL/rabbit were performed on days 56 and 58. Following ELISA titration of all bleeds and affinity purification of pooled bleeds from each rabbit, negative adsorption of antibodies against non-phosphorylated peptide (CGKKKRKLAKRIRE) was performed. Antibody was used at 1:200 in TBST + 1% BSA.

In Vitro Kinase Assays

Recombinant GST-$Drp1^{518–736}$ and GST-RalBP1 were purified from bacteria using glutathione-sepharose-4B (GE) and eluted with 15mM glutathione (Sigma). Proteins were dialyzed overnight in 2L elution buffer (100 mM Tris pH 8.0, 120 mM NaCl) and concentrated with an Amicon Ultra 10K centrifugal filter device (Millipore). For the *In vitro* kinase assay[2], α-cyclin B1 or α-RalBP1 immunoprecipitates or 25ng GST-CyclinB/Cdk1 (Cell Signaling Technologies) plus 0–1000ng GST-RalBP1 were suspended in protein kinase buffer (20 mM Hepes-KOH buffer, pH 7.4, 15 mM EGTA, and 20 mM $MgCl_2$) with 200ng of purified GST-$Drp1^{518–736}$, 50 μM ATP, γ^{32}P-ATP (hot kinase assay) and 1 μM

DTT for 30 min at 30°C. Samples were resolved by SDS-PAGE, and immunoblotted for phospho-S616-Drp1, Drp1, RalBP1 and Cdk1 (cold) or stained with Coomassie Brilliant Blue (Drp1 and RalBP1) followed by autoradiography for phospho-Drp1 (hot).

ATP Assay

Subconfluent HeLa cells were harvested in PBS, 0.5% Triton X-100, 2mM EDTA for 15 minutes on ice and 15μL of equivalent protein amounts were added to 135μL reaction buffer with 1mM DTT, 500μM D-luciferin and 1.25μg/mL firefly luciferase (ATP Determination Kit, Molecular Probes). 12 replicates were performed for each condition in a 96-well plate, including a no extract control. After 30 minute incubation at room temperature, luminescence was measured at 560nm on a Victor^3 luminometer (Perkin Elmer).

MTT Assay

HeLa cells were plated at 5000 cells per well in 3 × 96-well plates. At 24, 48 and 72 h, 50μL/well of 5mg/mL 3-(4,5-Dimethyl- 2-thiazolyl)-2,5-diphenyl-2H-tetrazolium bromide (MTT, Sigma) was added. After 4 hrs, cells were resuspended in 200μL DMSO. Absorbencies were recorded at 540 nm[32].

Immunofluorescence

Cells were plated on glass microslides the previous day, treated with 100nM MitoTracker Red CMXRos (Molecular Probes) for 30 minutes, fixed, permeabilized and either mounted immediately or incubated with Alexa-488 conjugated Phalloidin (1:50, Molecular Probes). Leica SP5 scanning confocal imaging system with Leica Pan Apochromat 100×/1.4–0.70 oil objective was used. A cell was judged to have fragmented mitochondria if greater than 90% of the mitochondria visible in the cell were punctate or circular and highly interconnected if less than 10% of the mitochondria were punctate or circular. >100 cells per cell type were blindly analyzed for three independent experiments[33].

Live Cell Imaging

HeLa cells expressing RFP targeted to the mitochondrial matrix (RFP-mito) were plated on 35mm glass bottom dishes and synchronized. Ten hours after release from thymidine live cell imaging was performed using Zeiss Axio Observer Z1 motorized imaging system with 100×/1.46 oil Plan Apochromat DIC objective and QuantEM backthinned EM-CCD camera. MetaMorph 7.6.5 software was used for image acquisition, movies and montages.

Analysis of Co-localization

Imaris software was employed for visualization and quantification of co-localization. Z-series images obtained from Leica SP5 scanning confocal imaging system were processed using the co-localization tool within Imaris. The GFP threshold was set to 0 and the MitoTracker red threshold was set to 80 to define the regions to be included or excluded from the co-localization analysis. The voxels meeting the selected criteria (thus identified as co-localized) were displayed as white voxels. Surface rendering of the GFP image and the co-localized image (GFP co-localized with the mitochondrial stain) was performed to determine the intensity sum per object. The percentage of GFP protein co-localized with

MitoTracker red was quantified by calculating the total of the intensity sum per object for the co-localized image divided by the total of the intensity sum per object for the GFP image.

Mitochondrial connectivity FRAP assay

HEK-TtH cells plated on glass-bottom plates in + 10% FBS were transiently transfected with YFP targeted to the mitochondrial matrix (mito-YFP). FRAP data collection and analysis was done using the Leica LAS AF FRAP-wizard software. Sixty RalA shRNA and scramble control HEK-TtH cells were evaluated in two independent experiments. A 240μm square was imaged with the 63× water-immersion objective (zoom 1.0) before and after a one iteration photobleach (488 nm laser) of a 4 μm circle placed over multiple mitochondria. Post-bleach recovery was evaluated with eighteen images recorded once every second post bleaching, with a total elapsed time of 18 seconds. Fluorescence was assessed at each time point for the FRAP region of interest and an unrelated background region. FRAP fluorescence data was normalized for background fluorescence and bleaching of the unrelated region, and graphed as a percentage of starting fluorescence. The mobile fraction of mito-YFP represents the ratio of recovered fluorescence to total fluorescence averaged for all cells assessed in one experiment[34]. Error bars indicate standard error of the mean within one experiment assessing 30 cells. *p* values were calculated using a paired two-tailed student's t-Test.

DSP Crosslinking and Co-IP

HeLa cells synchronized in M-phase (10 hours after last thymidine block) were incubated with 1mM dithiobis[succinimidylpropionate] (DSP, ThermoScientific) for 30 minutes at room temperature followed by addition of 10mM Tris pH 7.4 for 15 minutes. Cells were then lysed in solubilization buffer (50 mM Tris-HCL, pH 7.5, 1% digitonin)[19]. Crude mitochondrial and whole cell extracts extracts were prepared and endogenous RalA was immunoprecipitated from 400μg of extract using 0.75μg mouse anti-RalA monoclonal antibody (BD Transduction Laboratories). Input samples of 100 μg total protein isolated from uncrosslinked whole cell extracts or crude mitochondrial preparations were made alongside DSP-treated extracts.

RT-PCR

Reverse transcription of 2μg of total RNA was done with the Qiagen Omniscript RT kit using oligo-Dt priming. The resulting cDNA was diluted 1:25 and assessed by qPCR using SybrGreen PCR mastermix (Applied Biosystems) and the following Sec5 specific primers: 5'-GATCCTTCAGCTCATGCACA-3' (Forward) and 5'-GACTGAGATGGCCCAACAC-3' (Reverse). Reference primers for EEF1A1: 5'-GGATTGCCACACGGCTCACATT-3' (Forward) and 5'-GGTGGATAGTCTGAGAAGCTCTC-3' (Reverse) were used as controls. Measurements were done on the BioRad iCycler iQ (v3.1), with 40 amplification cycles. No RT control cDNA was included to ensure against contaminating transcript. For each sample, qPCR was done in triplicate, and the average of these values was used for ddCT analysis of relative transcript levels.

Statistical analysis

In each graph data represent mean ± S.D. of the indicated number (n) of independent experiments. Where indicated, statistical significance has been calculated by a Student t-test. P values are indicated in the legends

Supplementary Material

Refer to Web version on PubMed Central for supplementary material.

Acknowledgements

We thank S. Kornbluth for Drp1 plasmids, C. Freel, S. Johnson, Y. Gao and K. Norris for technical support, S. Issaq for the RalBP1-RalA fusion protein, S. Kornbluth, J. Rathmell, T.-P. Yao, C. Der, J. Kashatus and S. Horn for discussions and/or review of the manuscript. This work was supported by NIH grant CA94184 (C.M.C.). D.F.K. is a Leukemia and Lymphoma Society Fellow.

References

1. Detmer SA, Chan DC. Functions and dysfunctions of mitochondrial dynamics. Nat Rev Mol Cell Biol. 2007; 8:870–879. [PubMed: 17928812]
2. Taguchi N, Ishihara N, Jofuku A, Oka T, Mihara K. Mitotic phosphorylation of dynamin-related GTPase Drp1 participates in mitochondrial fission. J. Biol. Chem. 2007; 282:11521–11529. [PubMed: 17301055]
3. Camonis JH, White MA. Ral GTPases: corrupting the exocyst in cancer cells. Trends Cell Biol. 2005; 15:327–332. [PubMed: 15953551]
4. Feig LA. Ral-GTPases: approaching their 15 minutes of fame. Trends Cell Biol. 2003; 13:419–425. [PubMed: 12888294]
5. Wu JC, et al. Identification of V23RalA-Ser194 as a critical mediator for Aurora-A-induced cellular motility and transformation by small pool expression screening. J. Biol. Chem. 2005; 280:9013–9022. [PubMed: 15637052]
6. Lim KH, et al. Aurora-A phosphorylates, activates and relocalizes RalA. Mol. Cell. Biol. 2009
7. Bivona TG, et al. PKC regulates a farnesyl-electrostatic switch on K-Ras that promotes its association with Bcl-XL on mitochondria and induces apoptosis. Mol. Cell. 2006; 21:481–493. [PubMed: 16483930]
8. Poot M, et al. Analysis of mitochondrial morphology and function with novel fixable fluorescent stains. J. Histochem. Cytochem. 1996; 44:1363–1372. [PubMed: 8985128]
9. Hahn WC, et al. Creation of human tumour cells with defined genetic elements. Nature. 1999; 400:464–468. [PubMed: 10440377]
10. Bischoff JR, et al. A homologue of Drosophila aurora kinase is oncogenic and amplified in human colorectal cancers. EMBO J. 1998; 17:3052–3065. [PubMed: 9606188]
11. Neuspiel M, et al. Cargo-selected transport from the mitochondria to peroxisomes is mediated by vesicular carriers. Curr. Biol. 2008; 18:102–108. [PubMed: 18207745]
12. Roghi C, et al. The Xenopus protein kinase pEg2 associates with the centrosome in a cell cycle-dependent manner, binds to the spindle microtubules and is involved in bipolar mitotic spindle assembly. J. Cell Sci. 1998; 111(Pt 5):557–572. [PubMed: 9454730]
13. Smirnova E, Griparic L, Shurland DL, van der Bliek AM. Dynamin-related protein Drp1 is required for mitochondrial division in mammalian cells. Mol. Biol. Cell. 2001; 12:2245–2256. [PubMed: 11514614]
14. Pitts KR, Yoon Y, Krueger EW, McNiven MA. The dynamin-like protein DLP1 is essential for normal distribution and morphology of the endoplasmic reticulum and mitochondria in mammalian cells. Mol. Biol. Cell. 1999; 10:4403–4417. [PubMed: 10588666]
15. Smirnova E, Shurland DL, Ryazantsev SN, van der Bliek AM. A human dynamin-related protein controls the distribution of mitochondria. J. Cell Biol. 1998; 143:351–358. [PubMed: 9786947]

16. Tanaka A, et al. Proteasome and p97 mediate mitophagy and degradation of mitofusins induced by Parkin. The Journal of cell biology. 2010; 191:1367–1380. [PubMed: 21173115]
17. Lim KH, et al. Activation of RalA is critical for Ras-induced tumorigenesis of human cells. Cancer Cell. 2005; 7:533–545. [PubMed: 15950903]
18. Shipitsin M, Feig LA. RalA but not RalB enhances polarized delivery of membrane proteins to the basolateral surface of epithelial cells. Mol. Cell. Biol. 2004; 24:5746–5756. [PubMed: 15199131]
19. Otera H, et al. Mff is an essential factor for mitochondrial recruitment of Drp1 during mitochondrial fission in mammalian cells. The Journal of cell biology. 2010; 191:1141–1158. [PubMed: 21149567]
20. van de Weerdt BC, Medema RH. Polo-like kinases: a team in control of the division. Cell Cycle. 2006; 5:853–864. [PubMed: 16627997]
21. Rosse C, L'Hoste S, Offner N, Picard A, Camonis J. RLIP, an effector of the Ral GTPases, is a platform for Cdk1 to phosphorylate epsin during the switch off of endocytosis in mitosis. J. Biol. Chem. 2003; 278:30597–30604. [PubMed: 12775724]
22. Chen XW, Inoue M, Hsu SC, Saltiel AR. RalA-exocyst-dependent recycling endosome trafficking is required for the completion of cytokinesis. J. Biol. Chem. 2006; 281:38609–38616. [PubMed: 17028198]
23. Benard G, et al. Mitochondrial bioenergetics and structural network organization. J. Cell Sci. 2007; 120:838–848. [PubMed: 17298981]
24. Parone PA, et al. Preventing mitochondrial fission impairs mitochondrial function and leads to loss of mitochondrial DNA. PLoS One. 2008; 3:e3257. [PubMed: 18806874]
25. Hamad NM, et al. Distinct requirements for Ras oncogenesis in human versus mouse cells. Genes Dev. 2002; 16:2045–2057. [PubMed: 12183360]
26. Chien Y, et al. RalB GTPase-mediated activation of the IkappaB family kinase TBK1 couples innate immune signaling to tumor cell survival. Cell. 2006; 127:157–170. [PubMed: 17018283]
27. Stojanovski D, Koutsopoulos OS, Okamoto K, Ryan MT. Levels of human Fis1 at the mitochondrial outer membrane regulate mitochondrial morphology. J. Cell Sci. 2004; 117:1201–1210. [PubMed: 14996942]
28. Tyagi S, et al. Polo-like kinase1 (Plk1) knockdown enhances cisplatin chemosensitivity via up-regulation of p73alpha in p53 mutant human epidermoid squamous carcinoma cells. Biochem. Pharmacol. 2010; 80:1326–1334. [PubMed: 20655883]
29. Frank S, et al. The role of dynamin-related protein 1, a mediator of mitochondrial fission, in apoptosis. Dev Cell. 2001; 1:515–525. [PubMed: 11703942]
30. O'Hayer KM, Counter CM. A genetically defined normal human somatic cell system to study ras oncogenesis in vivo and in vitro. Methods Enzymol. 2006; 407:637–647. [PubMed: 16757358]
31. Freel CD, et al. Mitochondrial localization of Reaper to promote inhibitors of apoptosis protein degradation conferred by GH3 domain-lipid interactions. J. Biol. Chem. 2008; 283:367–379. [PubMed: 17998202]
32. Mosmann T. Rapid colorimetric assay for cellular growth and survival: application to proliferation and cytotoxicity assays. J. Immunol. Methods. 1983; 65:55–63. [PubMed: 6606682]
33. Benard G, Karbowski M. Mitochondrial fusion and division: Regulation and role in cell viability. Semin. Cell Dev. Biol. 2009; 20:365–374. [PubMed: 19530306]
34. Cleland MM, et al. Bcl-2 family interaction with the mitochondrial morphogenesis machinery. Cell Death Differ. 2011; 18:235–247. [PubMed: 20671748]

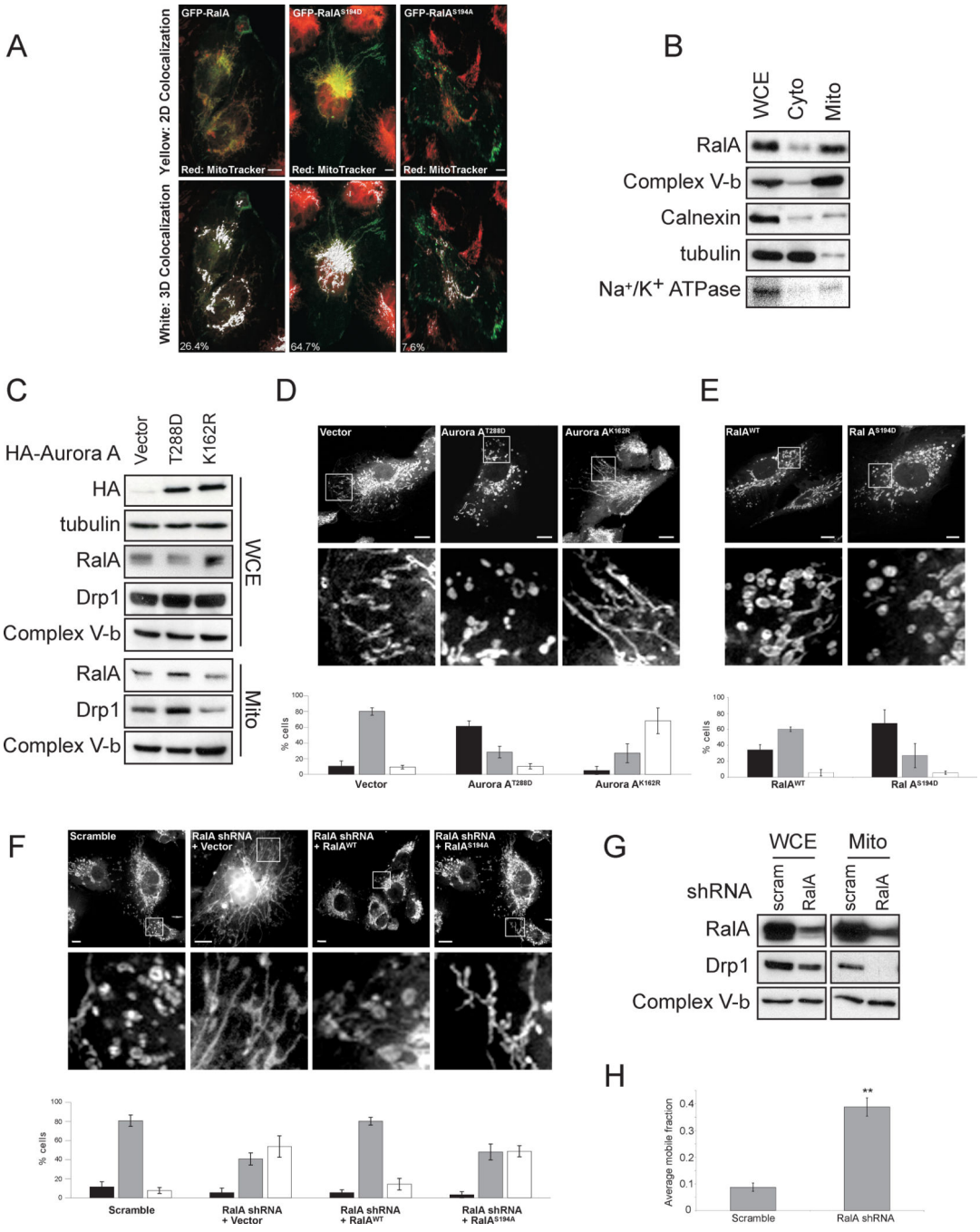

Figure 1.

Aurora A promotes RalA mitochondrial localization and fission. ***A*** HEK-TtH cells stably expressing GFP-tagged RalA, RalA^{S194D} or RalA^{S194A} were incubated with MitoTracker red to visualize mitochondria. GFP-RalA (green) and mitochondria (red) were visualized using confocal microscopy. A merge (yellow, 2D colocalization) and surface rendering (white, 3D co-localization) of the co-localization of GFP-RalA with mitochondria was determined with Imaris software. The percentage of GFP protein co-localized with MitoTracker red was quantified by calculating the total of the intensity sum per object for

the co-localized image divided by the total of the intensity sum per object for the GFP image. (scale bar = 5μm). ***B,C,G*** Immunoblot analysis of RalA and Drp1 levels in highly enriched mitochondrial fraction (mito), whole cell extracts (WCE) and when tested, cytoplasmic fraction (cyto) isolated from HEK-TtH cells expressing ***B*** no transgene, ***C*** vector, Aurora A^{T288D} or Aurora A^{K162R} or ***G*** scramble or RalA shRNA. Complex V-β (mitochondria), calnexin (ER), Na^+/K^+ ATPase (plasma membrane) and tubulin (cytoplasm) were analyzed to assess purity. Representative of 3 experiments. ***D,E,F*** Mitochondrial morphology visualized by MitoTracker Red staining of HEK-TtH cells expressing the indicated shRNAs and/or transgenes. Graph: % of cells (mean ± SD) exhibiting highly fragmented (■), intermediate (■) or highly interconnected (□) mitochondrial morphologies from 3 independent experiments (>100 cells). (scale bar = 5μm). ***H*** Mitochondrial network connectivity in HEK-TtH cells expressing scramble or RalA shRNA and transfected with mito-YFP. The normalized and photobleach corrected mobile fractions represent the mean ± SEM of 30 individual FRAP curves (** $p = 2.02 \times 10^{-8}$).

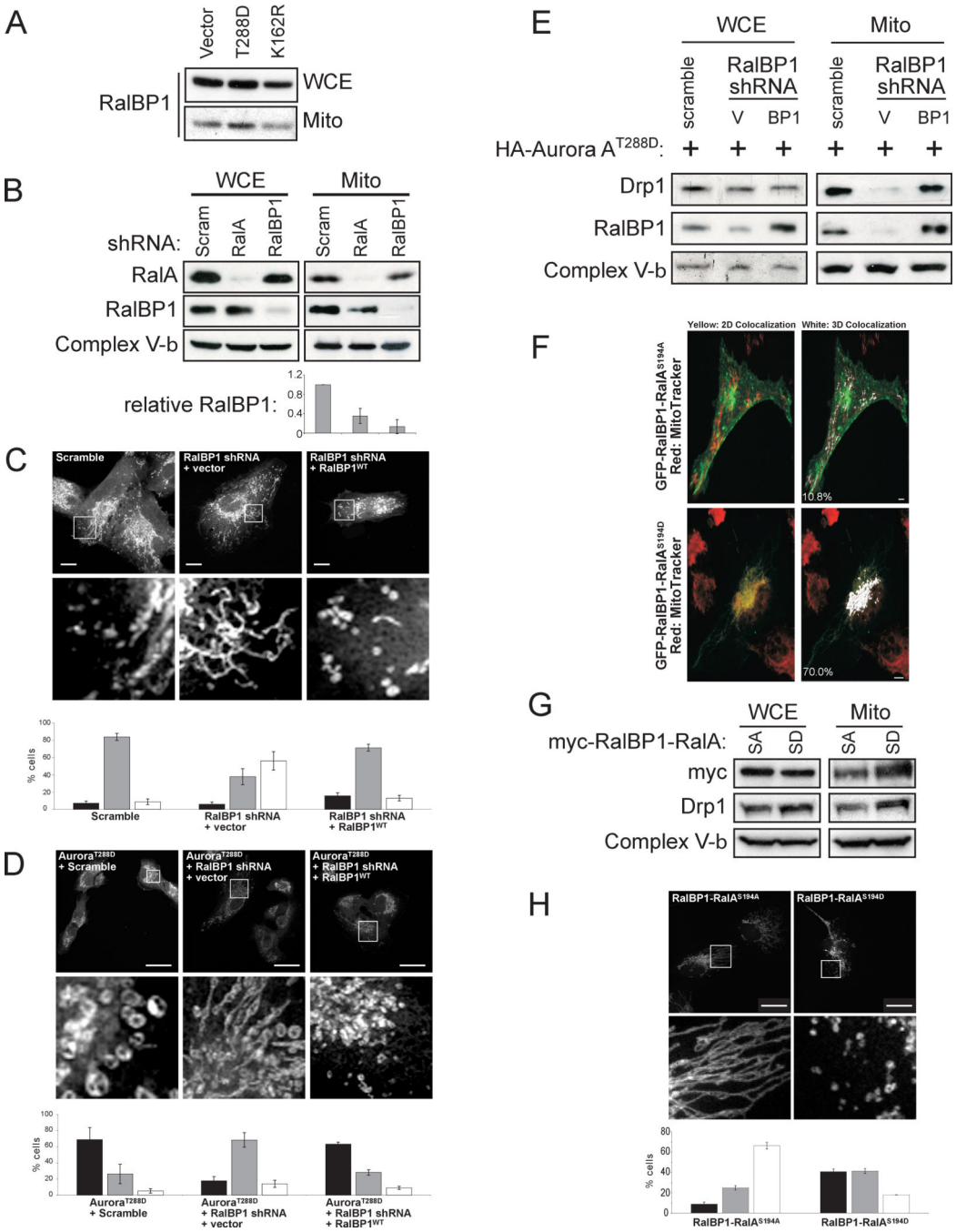

Figure 2.

RalBP1 promotes mitochondrial fragmentation. ***A,B,E,G*** Immunoblot analysis of RalA, RalBP1 or Drp1 levels in highly enriched mitochondrial fraction (mito) and whole cell extracts (WCE) isolated from HEK-TtH cells expressing ***A*** vector, Aurora A^{T288D} or Aurora A^{K162R}, ***B*** scramble control (scram), RalA shRNA or RalBP1 shRNA ***E*** Aurora A^{T288D} plus either scramble control or RalBP1 shRNA complemented with vector (V) or shRNA-resistant RalBP1 (BP1) or ***G*** myc-RalBP1-$RalA^{S194A}$ or myc-RalBP1-$RalA^{S194D}$. Complex V-β (mitochondria) was analyzed to assess purity. Representative of 3 experiments. ***C,D,H***

Mitochondrial morphology visualized by MitoTracker Red staining of ***C*** HEK-TtH cells, ***D*** HEK-TtH cells expressing active Aurora A^{T288D} and a scramble sequence or RalBP1 shRNAs alone or in conjunction with shRNA-resistant wild type RalBP1 or ***H*** HEK-TtH cells expressing Myc-RalBP1-$RalA^{S194A}$ or Myc-RalBP1-$RalA^{S194D}$. Graph: % of cells (mean ± SD) exhibiting highly fragmented (■), intermediate (■) or highly interconnected (□) mitochondrial morphologies from 3 independent experiments (>100 cells) (scale bar = ***C*** 5μm ***D,H*** 25μm). ***F*** Overlap (merge, yellow) of the distribution of GFP-RalBP1-$RalA^{S194A}$ or GFP-RalBP1-$RalA^{S194D}$, as detected by immunofluoresence of GFP (green), and MitoTracker red-positive mitochondria (red) in HEK-TtH cells. Surface rendering of the co-localization of GFP-RalBP1-RalA fusion proteins with mitochondria (white) was determined with Imaris software. The percentage of GFP protein co-localized with mitotracker red was quantified by calculating the total of the intensity sum per object for the co-localized image divided by the total of the intensity sum per object for the GFP image. (scale bar = 5μm for SD or 3μm for SA).

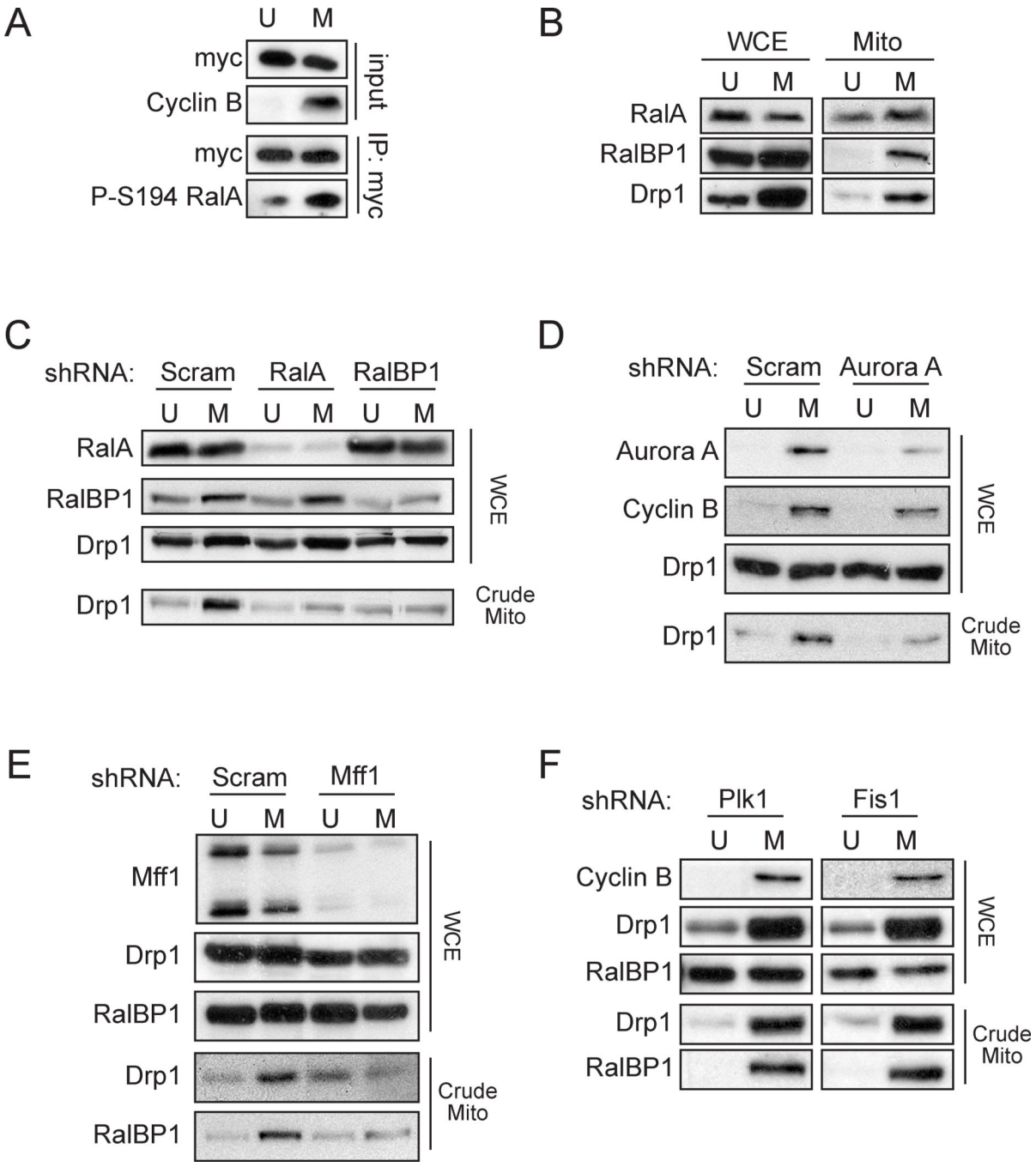

Figure 3.

RalA and RalBP1 promote mitochondrial localization Drp1. ***A*** Extracts isolated from HeLa cells expressing myc-RalA, either unsynchronized (U) or synchronized in mitosis (M) using double thymidine block were either analyzed by immunoblot for levels of myc-RalA and cyclin B or subjected to immunoprecipitation (IP) with antibodies against myc and analyzed by immunoblot for levels of myc-RalA or phospho-S194 RalA. Representative of 3 experiments. ***B*** Immunoblot analysis of RalA, RalBP1 and Drp1 levels in mitochondrial fractions (mito) and whole cell extracts (WCE) isolated from HeLa cells either

unsynchronized (U) or synchronized in mitosis (M) using double thymidine block. Representative of 3 experiments. ***C–F*** Immunoblot analysis of RalA, RalBP1, Drp1, Cyclin B, Aurora A and Mff1 levels in crude mitochondrial fractions (mito) and whole cell extracts (WCE) isolated from HeLa cells, either unsynchronized (U) or synchronized in mitosis (M) using double thymidine block, and expressing ***C*** scramble control, RalA shRNA or RaBP1 shRNA or ***D*** doxycycline inducible scramble control or Aurora A shRNA ***E*** scramble control or Mff1 shRNA or ***F*** Plk1 or Fis1 shRNA. Representative of 3 experiments.

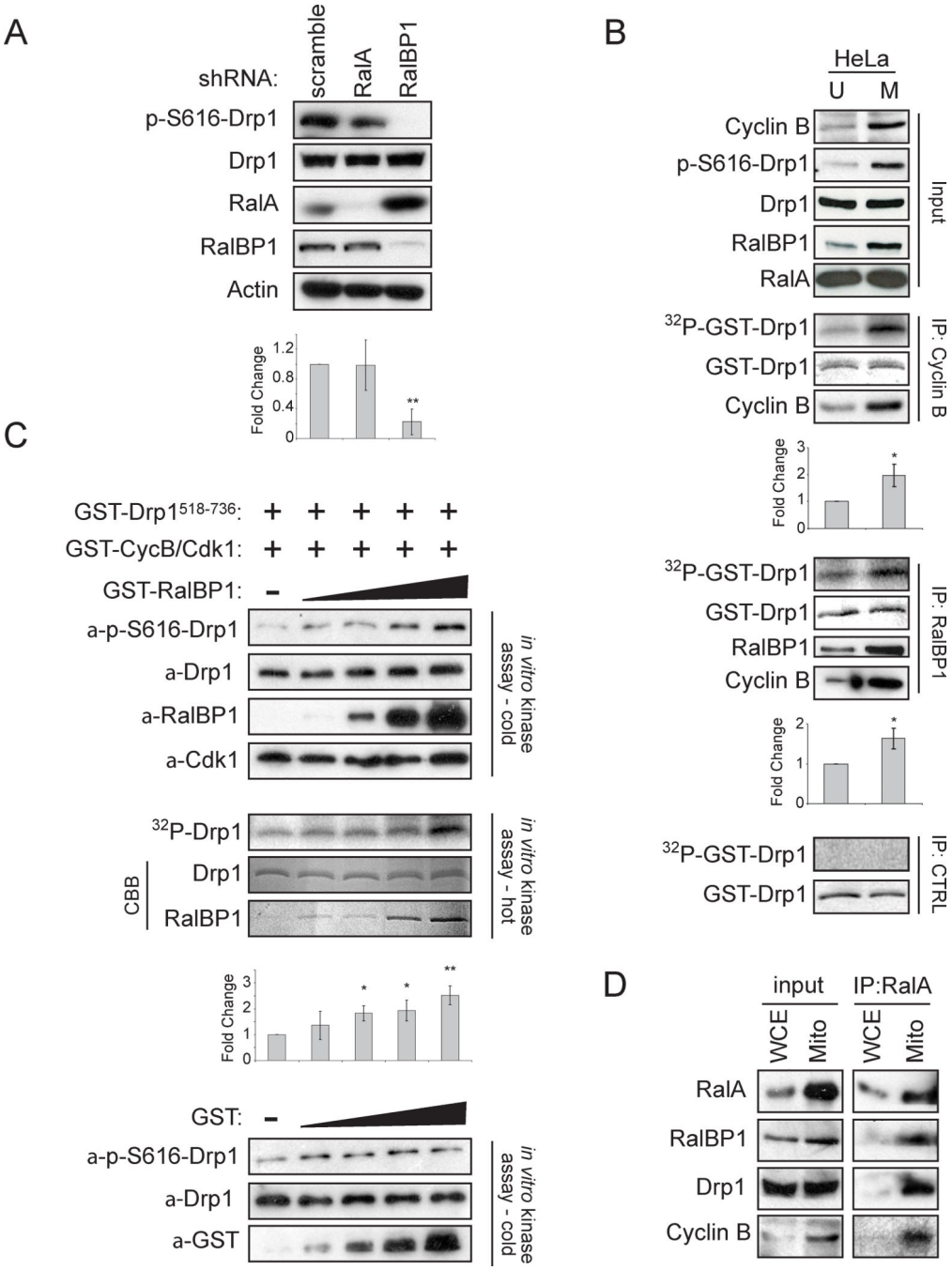

Figure 4.

RalBP1 promotes phosphorylation of Drp1. ***A*** Immunoblot analysis of S616 phosphorylated (p-S616-Drp1), Drp1, RalA, RalBP1 and actin levels in HeLa cells expressing a scramble control, RalA shRNA or RalBP1 shRNA. Graph represents mean p-S616-Drp1 signal intensity measured by imageJ from 3 experiments +/− SD (** $p = 0.008$). ***B*** Extracts isolated from HeLa cells, either unsynchronized (U) or synchronized in mitosis (M) using double thymidine block were either analyzed by immunoblot for levels of RalA, Drp1, cyclin B or S616 phosphorylated Drp1, or subjected to immunoprecipitation (IP) with either no antibody

or antibodies against cyclin B or RalBP1, followed by incubation with GST-Drp1 and γ^{32}P-ATP, and resolved on an acrylamide gel. ^{32}P-labeled GST-Drp1 was visualized by phosphorimager while total GST-Drp1 was visualized by coomassie brilliant blue staining. Graphs represent mean ^{32}P-GST-Drp1 signal intensity measured by imageJ from 3 experiments +/− SD (* $p = 0.028$ for Cyclin B, 0.027 for RalBP1). ***C*** 200ng GST-Drp1 and 25ng GST-Cyclin B/Cdk1 were incubated with increasing amounts of either GST-RalBP1 or GST (0, 125, 250, 500, 1000ng) in addition to either ATP or γ^{32}P-ATP. Reactions were resolved by SDS-PAGE and either subjected to immunoblot for Drp1, RalBP1 and S585 phosphorylated Drp1 (cold kinase assay) or visualized by phosphorimager (hot kinase assay). GST, GST-Drp1 and GST-RalBP1 were visualized by coomassie brilliant blue staining (CBB). Graph represents mean p-S616-Drp1 signal intensity measured by imageJ from 3 experiments +/− SD (* $p = 0.020$, 0.028 ** $p = 0.009$). ***D*** Immunoblot analysis of RalA, RalBP1, Drp1 and Cyclin B levels in crude mitochondrial fractions (mito) and whole cell extracts (WCE) isolated from HeLa cells synchronized in mitosis (M) using double thymidine block, treated with DSP, and subjected to immunoprecipitation with and anti-RalA antibody.

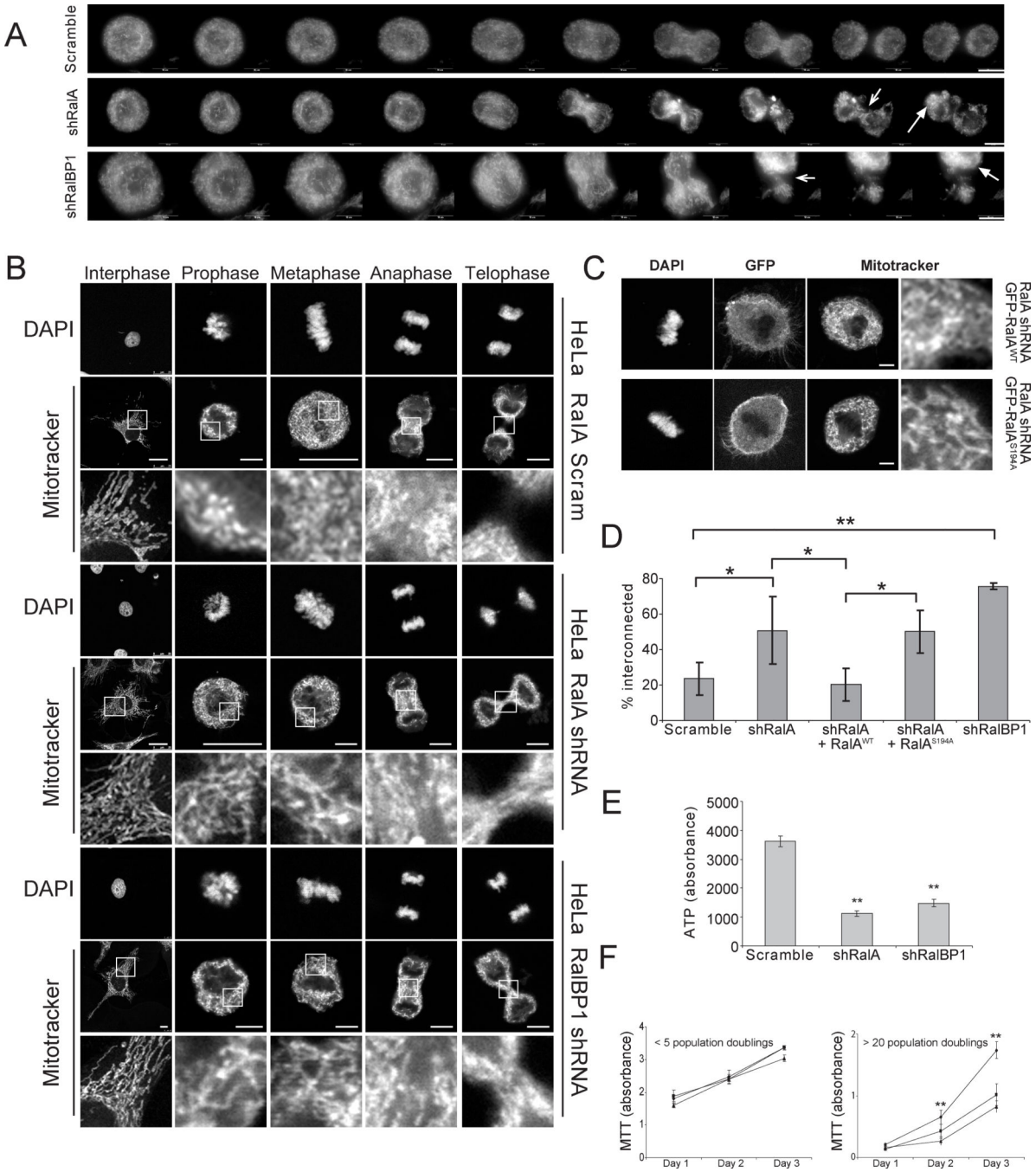

Figure 5.

Knockdown of RalA or RalBP1 prevents mitosis-induced mitochondrial fission. ***A*** Mitochondrial morphology as visualized by live cell imaging of HeLa cells stably expressing RFP-Mito and scramble control, RalA shRNA or RalBP1 shRNA after release from double thymidine block. Arrows (1, 2) indicate regions of mitochondria retained during telophase and (3, 4) unequal distribution of mitochondria to daughter cells (scale bar = 10μm). ***B*** Mitochondrial morphology visualized by MitoTracker Red staining of HeLa cells expressing a scramble control, RalA shRNA or RalBP1 shRNA at the indicated phases

of mitosis upon being synchronized in mitosis using double thymidine block. DAPI staining was used to assign mitotic phase (scale bar = 25μm for scram interphase and metaphase and RalA interphase and prophase, 10μm for scram anaphase and telophase and RalBP1 interphase and 7.5μm for all other images). ***C*** Mitochondrial morphology HeLa cells expressing RalA shRNA complemented with GFP-tagged, shRNA resistant RalA in the wild type (WT) or S194A mutant configuration and captured at metaphase (DAPI) (scale bar = 10μm). ***D*** Quantitation of the percent of cells (mean ± SD, n = 3 independent experiments with ≥ 30 cells analyzed per condition) exhibiting mitochondrial elongation during metaphase. (* $p \leq 0.05$, ** $p \leq 0.01$) ***E*** ATP production of HeLa cells stably expressing scramble, RalA or RalPB1 shRNA was determined by measuring ATP-dependent luciferase activity measured at 560nm on a Victor^3 luminometer. (The experiments were repeated at least 3 times, and each time the error was calculated from 12 replicates, ** $p = 1.6 \times 10^{-7}$ for RalA, 5.3×10^{-7} for RalBP1). ***F*** Proliferation of HeLa cells stably expressing scramble (◆), RalA (■) or RalBP1 (▲) as measured by MTT assay. Measurements were performed over three days using cells with fewer than 5 or greater than 20 population doublings following selection for the transgene. (The experiments were repeated at least 3 times, and each time the error was calculated from 16 replicates; day 2: ** $p = 4.5 \times 10^{-5}$ for RalA, 6.3×10^{-5} for RalBP1, day 3: ** $p = 4.5 \times 10^{-8}$ for RalA, 2.7×10^{-6} for RalBP1)